Nanoscale Research Letters

NANO EXPRESS

Open Access

Threshold Switching of Ag-Ga_2Te_3 Selector with High Endurance for Applications to Cross-Point Arrays

Jaeyeon Kim, Jimin Lee, Minkyu Kang and Hyunchul Sohn*

Abstract

Threshold switching in chalcogenides has attracted considerable attention because of their potential application to high-density and three-dimensional stackable cross-point array structures. However, despite their excellent threshold switching characteristics, the selectivity and endurance characteristics of such selectors should be improved for practical application. In this study, the effect of Ag on the threshold switching behavior of a Ga_2Te_3 selector was investigated in terms of selectivity and endurance. The Ag-Ga_2Te_3 selector exhibited a high selectivity of 10^8 with low off-state current of < 100 fA, steep turn-on slope of 0.19 mV/dec, and high endurance of 10^9 cycles. The transient response was verified to depend on the pulse input voltage and measurement temperature. Considering its excellent threshold switching characteristics, the Ag-Ga_2Te_3 selector is a promising candidate for applications in cross-point array structures.

Keywords: Thin films, Vapor deposition, Diffusion, Electronic properties, TEM

Introduction

Resistive random-access memory has been investigated as a promising candidate for next-generation nonvolatile memory, owing to its simple operation, low power consumption, three-dimensional (3D) stackable potential, scalability, and simple structure [1–4]. However, the sneak current passing through adjacent cells must be reduced to avoid the potential operation failure that can occur in 3D cross-point array (CPA) structures with high cell density [5, 6]. Two-terminal selector devices with low off-state currents and high on/off ratios are favored to address such sneak current issues [7, 8].

Various types of selector devices with threshold switching (TS) characteristics have been proposed previously, including Ovonic threshold switch (OTS) [9], metal–insulator transition (MIT) [10], field-assisted superlinear threshold switch (FAST) [11], electrochemical metallization (ECM) [12], and mixed-ionic-electronic conduction (MIEC) [13]. However, the selectivity and leakage current of OTS and MIT selectors should be improved for practical applications [9, 10]; the nature of materials used for FAST selectors is not known [11]. Meanwhile, ECM and MIEC devices with Ag or Cu have attracted considerable attention because of their desirable TS characteristics, including their low leakage current, high on/off ratio, steep turn-on slope, and large hysteresis between the threshold voltage (V_{TH}) and hold voltage (V_{Hold}) [14–16]. In a one-selector-one resistor (1S1R) structure, the voltage window for the read operation is determined by the set voltage (V_{Set}) of the memory and V_{TH} of the selector. Because V_{Set} varies according to the materials used for the memory device, the modulation of V_{TH} is required to facilitate the operation of a 1S1R device [17]. Moreover, the large difference between V_{TH} and V_{Hold} can alleviate the operational complexity of a CPA structure and relax the stringent voltage-matching requirements [18, 19].

*Correspondence: hyunchul.sohn@yonsei.ac.kr
Department of Materials Science and Engineering, Yonsei University, 03722 Seoul, Republic of Korea

The switching mechanism of such selector devices using an active metal, such as Ag or Cu, is based on the formation and dissolution of the metallic conduction channel. Therefore, the matrix of the electrolyte material significantly affects the migration of the active metal and switching speed of the selector. The switching speed of a selector based on an oxide-based electrolyte is generally slower than the order of microseconds [20–22], which is relatively slow when compared with that of previously reported OTS [23] or MIT selector devices [24]. Meanwhile, defects in chalcogenide films, such as nonbonded Te (NBT), can lower the activation energy for the migration of active metal ions; therefore, chalcogenide materials are preferable for the fast migration of active metal ions [18]. However, because of their randomly formed metallic conduction channel, these materials have disadvantages in terms of their switching endurance characteristic, which is a crucial factor for selectors [14, 18, 25]. The endurance of an ECM device can be improved from 10^3 to 10^6 cycles using an intermediate buffer layer [26]. However, further endurance improvement is required for practical applications of such devices in CPA structures [5].

In this study, a highly defective amorphous Ga_2Te_3 was used as a switching layer by inserting an Ag layer to investigate the TS characteristics in terms of a low leakage current (off-state current), high selectivity, modulation of V_{TH} and V_{Hold}, and high endurance. Amorphous Ga_2Te_3 is advantageous as an electrolyte material because there are several NBTs that lower the activation energy of Ag migration and Ga vacancy, which acts as a migration site for Ag in amorphous Ga_2Te_3 films [27–29].

Methods

Selector devices of TiN/Ag/Ga_2Te_3/TiN stacks were fabricated with a via-hole structure to investigate their TS characteristics, as depicted in Figure 1a. First, TiN plugs with a size of 0.42 μm × 0.42 μm were formed as the bottom electrodes (BEs). Ga_2Te_3 thin films with thicknesses of 40 nm were deposited through RF magnetron co-sputtering using Ga_2Te and Te targets. Subsequently, an Ag film with a thickness of 10 nm was deposited on Ga_2Te_3 films through DC magnetron sputtering. Finally, a TiN top electrode (TE) was formed using DC magnetron sputtering and a lift-off method.

The electrical properties were investigated using a Keysight B1500A analyzer at 298 K. DC switching tests were conducted with a compliance current (I_{comp}) to avoid the hard breakdown of TS devices. In addition, AC $I-V$ measurements were conducted with an external load resistance of 1 MΩ to prevent the breakdown of devices. The microstructure of the device was investigated using transmission electron microscopy (TEM; JEOL FEM-F200), as shown in Fig. 1b. The cross-sectional TEM samples of devices were prepared using a focused ion beam system. The atomic distribution of Ag in the Ga_2Te_3 film was investigated using TEM-energy dispersive spectroscopy (EDS) measurements.

Results and Discussion

Figure 2a shows a cross-sectional TEM image of the pristine TiN/Ag-Ga_2Te_3/TiN stack of a selector device. The Ag interlayer with a thickness of 10 nm was not observed on top of the Ga_2Te_3 thin film. Figure 2b presents the EDS mapping of the Ga, Te, Ag, and Ti elements for the red rectangular region marked in Fig. 2a. The EDS mapping images show that Ag is uniformly distributed in the Ga_2Te_3 film even though a co-sputtering process of Ag was not applied. The homogeneous Ag-Ga_2Te_3 film may have been formed probably because of the diffusion of Ag during the stack formation. Such fast homogenization of Ag was also reported for the GeTe films [30–32]. Ag may diffuse into the Ga_2Te_3 thin film owing to defects such

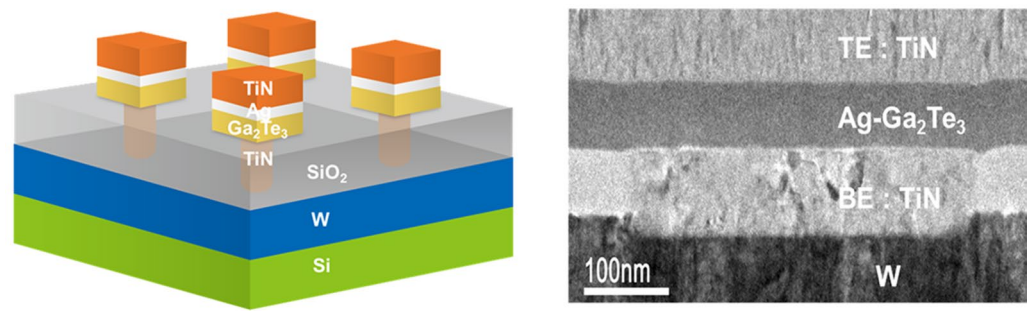

Fig. 1 **a** Schematic of the Ag/Ga_2Te_3 selector devices. **b** Cross-sectional TEM image of the TiN/Ag-Ga_2Te_3/TiN selector device

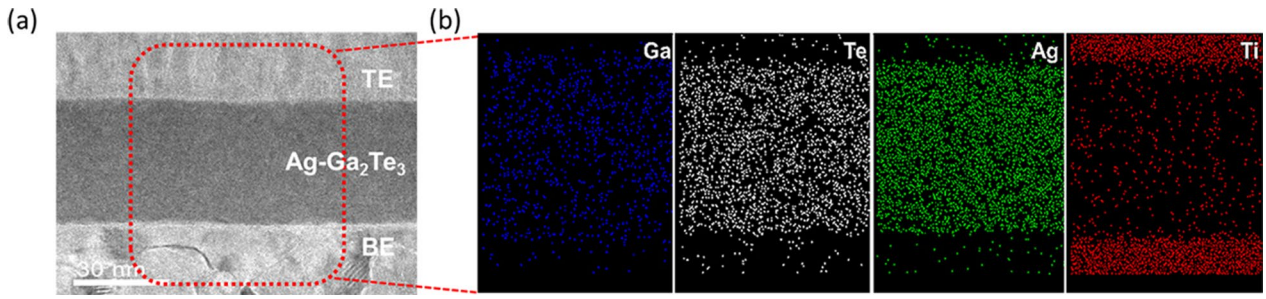

Fig. 2 **a** Cross-sectional TEM image of the TiN/Ag-Ga_2Te_3/TiN device structure. **b** TEM–EDS mapping images of Ga, Te, Ag, and Ti for the red rectangular region marked in **a**

as NBT and Ga vacancies in the Ga_2Te_3 thin films [18, 27–29].

Figure 3a shows the current−voltage (I−V) characteristics of the Ag-Ga_2Te_3 devices with a bottom electrode area of 0.42 μm × 0.42 μm for 100 consecutive cycles of DC sweeps. The device showed TS characteristics without a forming process. When the voltage on TE swept from 0 to 1.5 V, the conduction current increased abruptly at the $V_{TH} \approx 0.87$ V to I_{comp} that was set to 1 μA, which indicated that the device switched from a high-resistance state (HRS) to a low-resistance state (LRS). The device relaxed back to the HRS at $V_{Hold} \approx 0.12$ V when the voltage was reduced from 1.5 to 0 V, demonstrating a considerable difference between V_{TH} and V_{Hold}. The off-state current at V_{TH} was measured to be less than 100 fA, which corresponds to one of the lowest values when compared to previously reported chalcogenide-based selectors using active metals such as Ag or Cu [14, 18, 25, 30, 33]. The selectivity, which is defined as the ratio of the on-state current to the off-state current, was approximately 10^8. As shown in Fig. 3b, the I−V curves showed stable TS characteristics for various I_{comp} values ranging from 10 nA to 10 μA, indicating its flexibility in the operation current. The forming-free TS with a large difference between V_{TH} and V_{Hold} of the Ag-Ga_2Te_3 selector devices are distinctly favorable over the TS characteristics of the Ga_2Te_3-only OTS selector devices [34]. Because the forming process is considered as a potential obstacle for real device applications, the forming-free characteristics of the Ag-Ga_2Te_3 device are more favorable than selector device, which requires a forming process [35]. Further, the TS characteristic with a large hysteresis of the Ag-Ga_2Te_3 selector device may lower the operational complexity of the CPA structure and ease the stringent voltage-matching requirements [18, 19]. Additionally, the Ag-Ga_2Te_3 selector shows a steep turn-on slope of 0.19 mV/dec with a scan rate of 1.5 mV per measurement step, as shown in Fig. 3c. The Ag-Ga_2Te_3 selector device demonstrated excellent characteristics including its high selectivity (10^8), low off-state current (<100 fA), steep turn-on slope (0.19 mV/dec), and forming-free characteristics.

As variation in device performance is a crucial factor for the application of a selector to a CPA structure, the distributions of V_{TH}, V_{Hold}, resistance of the high-resistance state (R_{HRS}), and resistance of the low-resistance state (R_{LRS}) were investigated for 25 random devices. Figure 4a shows that the distribution of the threshold voltage ranged from 0.75 to 1.08 V, while the hold voltage distribution ranged from 0.06 to 0.375 V. In addition, the

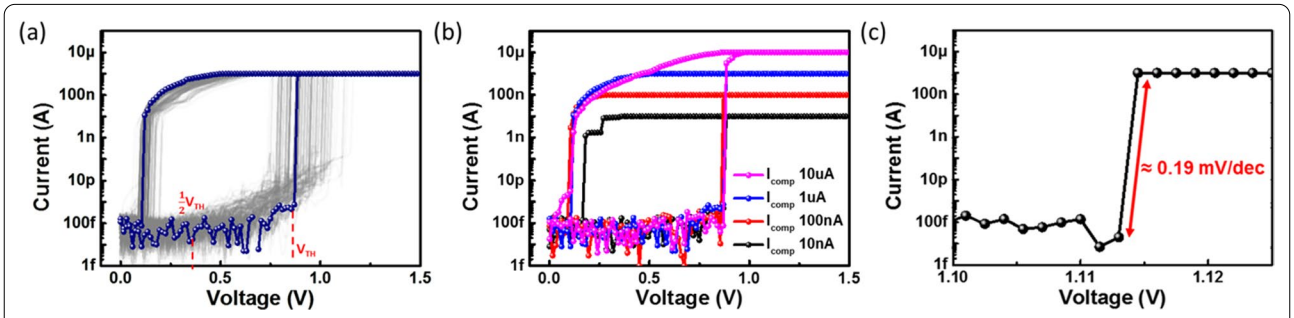

Fig. 3 **a** *I–V* characteristics of the Ag-Ga_2Te_3 selector device for DC voltage sweep results during 100 consecutive cycles. The Ag-Ga_2Te_3 selector device shows significantly low leakage current (< 100 fA) with an on/off ratio of 10^8. **b** TS characteristics of the Ag-Ga_2Te_3-based selector device at various I_{comp} values from 10 nA to 10 μA. **c** Close-up view of the *I–V* curve at TS that shows a turn-on slope of 0.19 mV/dec

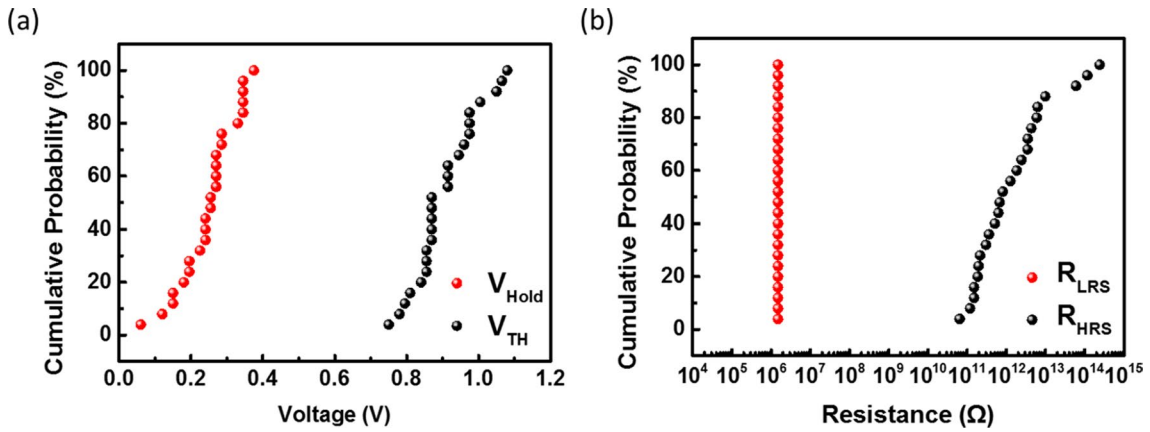

Fig. 4 **a** Device-to-device variations of V_{TH} and V_{Hold} for 25 devices. **b** Device-to-device variations of R_{HRS} and R_{LRS} for 25 devices

resistance distribution at the HRS ranged from 10^{11} to 10^{14} Ω, while the resistance at the LRS was approximately 10^6 Ω, as shown in Fig. 4b. Owing to the metal conduction channel formation, selector devices using active metals such as Ag or Cu exhibit relatively wide variation characteristics [36, 37]. Accordingly, studies on improving the reliability of these characteristics via doping or buffer layer insertion have been reported [37, 38].

To investigate the transient response of the Ag-Ga_2Te_3 selector, the current was measured using a waveform generator fast measurement unit (WGFMU) during a voltage pulse with a height of 3 V, rising−falling time of 100 ns, and duration of 1.5 μs with an external load resistance of 1 MΩ, as shown in Figure 5a. The conduction current of the Ag-Ga_2Te_3 selector device reached its peak value after 406 ns from the point at which the voltage reached its maximum of 3 V. Furthermore, the device was switched to the off-state within 605 ns after the applied voltage was removed. Hence, the switching-on time and switching-off time of the Ag-Ga_2Te_3 selector were estimated to be approximately 400 ns and 600 ns, respectively. The slow switching of the Ag-Ga_2Te_3 selector can be attributed to the migration and redox reactions of Ag for the formation of the conduction channel. In addition, the influence of the applied voltage and measurement temperature on the switching time was investigated with an input voltage of 1.5−5 V and at a measurement temperature of 298−375 K. The switching-on time was decreased from 1 μs to 294 ns, whereas the switching-off time was increased from 400 ns to 849 ns as the pulse voltage was increased from 1.5 to 3.5 V, as shown in Fig. 5b. The dependence of the switching speed on the applied voltage is comparable with the previously reported results of Ag layer on HfO_2 and TiO_2 [39]. Moreover, Fig. 5c shows that the switching-on and switching-off times decreased with increasing measurement temperature. According to the Arrhenius plot of switching speed against measurement temperature shown in Fig. 5d, the exponential dependence of switching speed on measurement temperature can be attributed to thermally facilitated processes, such as the diffusion of Ag atoms in the electrolyte film matrix [40]. The activation energies for switching-on and switching-off were estimated to be 0.50 eV and 0.40 eV, respectively, which are comparable with those presented in a previous report on a Ag filament-based device [41]. It was reported that the Ag conductive channels were formed under electrical bias in HfO_2, SiO_2, and TiO_2 [15, 42, 43]. However, in this study, Ag was observed to be uniformly distributed in pristine Ga_2Te_3 films. Although the mechanism for TS in Ga_2Te_3 films with uniform distribution of Ag is not clearly understood, Ag may be related to the formation of conductive channels in Ga_2Te_3 films under electrical bias. Therefore, the dependence of switching speed on the input voltage and measurement temperature of the Ag-Ga_2Te_3 selector device can be attributed to the formation of the conductive channels.

The AC endurance characteristic was investigated under the same voltage pulse condition as that of the switching speed test. The reading voltages for the HRS and LRS were 0.5 and 3 V, respectively. The measured resistances of the HRS and LRS were plotted for 450 points per decade, as shown in Fig. 6. The Ag-Ga_2Te_3 selector device exhibited stable endurance characteristics up to 10^9 cycles maintaining a selectivity of 10^8, thus demonstrating excellent switching endurance characteristics when compared with those of other selectors that utilized chalcogenide and active metals [18, 25, 30].

Conclusions

In this study, we demonstrated the stable TS characteristics of a selector device fabricated using Ag with high ion mobility and highly defective amorphous Ga_2Te_3 as

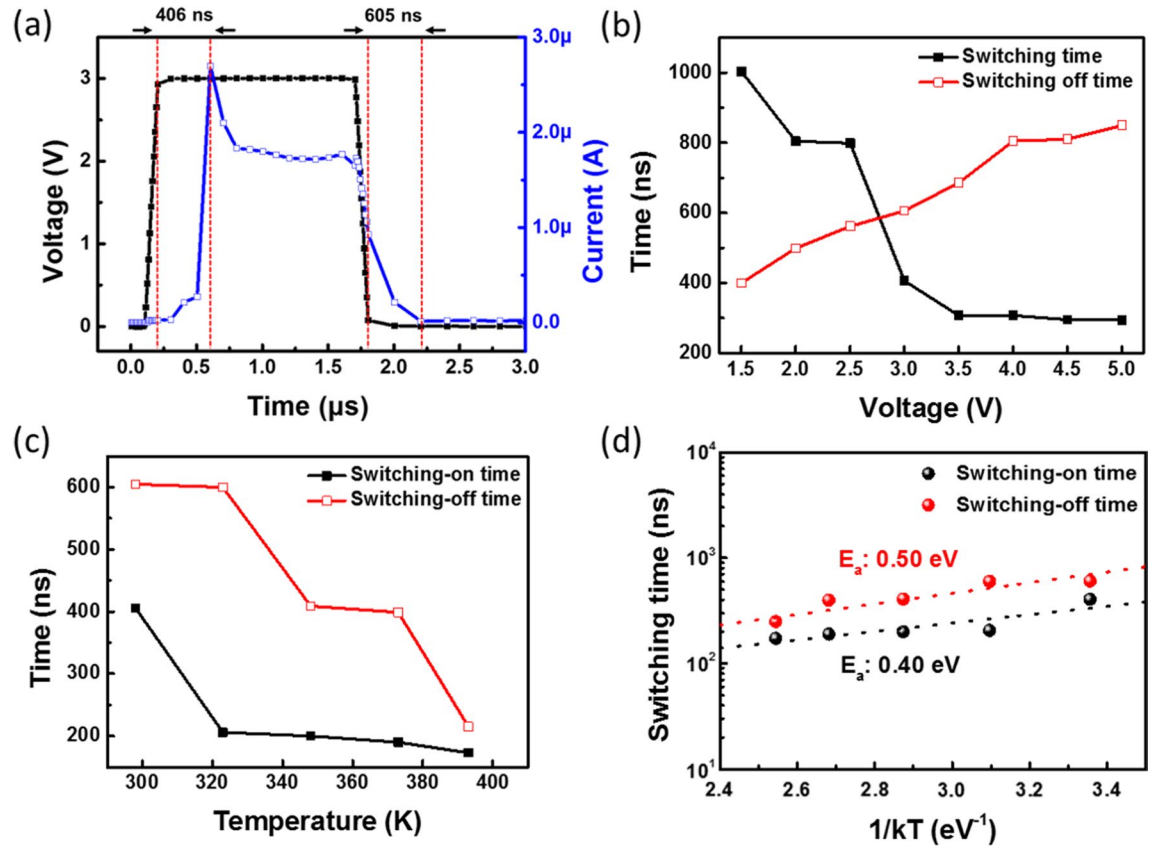

Fig. 5 **a** AC *I–V* measurement of the Ag-Ga_2Te_3 selector device (measurement conditions: rising time = 100 ns, duration = 1.5 μs, falling time = 100 ns, and input voltage = 3 V). **b** Switching speed dependence on applied pulse voltage. **c** Switching speed dependence on measurement temperature. **d** Arrhenius plot of switching speed against measurement temperature

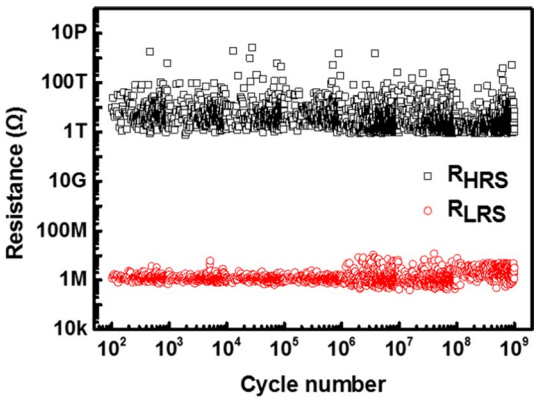

Fig. 6 AC endurance characteristic of the Ag-Ga_2Te_3 selector device up to 10^9 cycles (0.5 V and 3 V reading voltages for R_{HRS} and R_{LRS}, respectively)

a switching layer. TEM analyses of the TiN/Ag-Ga_2Te_3/TiN structure showed that the embedded Ag interlayer was completely diffused into the Ga_2Te_3 film to produce uniform Ag distribution in the Ga_2Te_3 layer. This may be because of the highly defective structure of amorphous Ga_2Te_3 during subsequent TE TiN deposition. The Ag-Ga_2Te_3 selector device exhibited forming-free TS, a large hysteresis (1 V), high selectivity (10^8), low off-state current (<100 fA), steep turn-on slope (0.19 mV/dec), and excellent endurance characteristics (10^9 cycles). In addition, AC I−V measurements showed the switching speed to be in the order of hundreds of nanoseconds. The dependence of switching speed on pulse voltage may be the combined effect of Ag migration and redox reaction. Moreover, the Arrhenius behavior of switching speed based on the measurement temperature suggested that the TS is related to a thermally facilitated process. In conclusion, the Ag-Ga_2Te_3 device with the excellent TS and endurance characteristics is a promising candidate for selector in the CPA memory applications.

Abbreviations

3D: 3-Dimensional; CPA: Cross-point array; TS: Threshold switching; OTS: Ovonic threshold switch; MIT: Metal–insulator transition; FAST: Field-assisted

super-linear threshold switch; ECM: Electrochemical metallization; MIEC: Mixed-ionic-electronic conduction; V_{TH}: Threshold voltage; V_{Hold}: Hold voltage; 1S1R: One selector-one resistor; V_{set}: Set voltage; NBT: Non-bonded Te; TE: Top electrode; BE: Bottom electrode; I_{comp}: Compliance current; HRS: High-resistance state; LRS: Low-resistance state; R_{HRS}: Resistance of the high-resistance state; R_{LRS}: Resistance of the low-resistance state.

Acknowledgements
This work was supported by the Ministry of Trade, Industry & Energy, Korea, under the Industrial Strategic Technology Development Program (Grant No. 20010569).

Authors' Contributions
JYK and MKK fabricated and characterized the Ag-Ga_2Te_3-based selector devices. JYK and JML designed the electrical measurements for threshold switching. JYK wrote the manuscript. HSS supervised the whole work. All authors critically read and approved the final manuscript.

Availability of Data and Materials
All data are fully available without restriction.

Declarations

Competing interests
There are no conflicts to declare.

Received: 24 May 2021 Accepted: 29 July 2021
Published online: 09 August 2021

References

1. Akinaga H, Shima H (2010) Resistive random access memory (ReRAM) based on metal oxides. Proc IEEE 98(12):2237–2251. https://ieeexplore.ieee.org/document/5607274
2. Wong HSP, Lee H-Y, Yu S, Chen Y-S, Wu Y, Chen P-S et al (2012) Metal-oxide RRAM. Proc IEEE 100(6):1951–1970. https://doi.org/10.1109/jproc.2012.2190369
3. Lee K, Kim J, Mok I-S, Na H, Ko D-H, Sohn H et al (2014) RESET-first unipolar resistance switching behavior in annealed Nb2O5 films. Thin Solid Films 558:423–429. https://doi.org/10.1016/j.tsf.2014.03.003
4. Yu S (2016) Resistive Random Access Memory (RRAM). Synth Lect Emerg Eng Technol 2(5):1–79. https://doi.org/10.2200/S00681ED1V01Y201510EET006
5. Aluguri R, Tseng T (2016) Notice of violation of IEEE publication principles: overview of selector devices for 3-D stackable cross point RRAM arrays. IEEE J Electron Device 4(5):294–306. https://doi.org/10.1109/JEDS.2016.2594190
6. Burr GW, Shenoy RS, Virwani K, Narayanan P, Padilla A, Kurdi B et al (2014) Access devices for 3D crosspoint memory. J Vac Sci Technol B, Nanotechnol Microelectron: Mater Proc Meas Phenomena. https://doi.org/10.1116/1.4889999
7. An Chen (2013) Emerging memory selector devices. Non-Volatile Memory Technology Symposium (NVMTS). https://doi.org/10.1109/NVMTS.2013.6851049.
8. Song J, Koo Y, Park J, Lim S, Hwang H (2019) Selector devices for x-point memory. In: Adv Non-Volatile Memory Storage Technol, 2nd edn, pp 365–390. https://doi.org/10.1016/B978-0-08-102584-0.00011-5.
9. Lee MJ, Lee D, Cho SH, Hur JH, Lee SM, Seo DH et al (2013) A plasma-treated chalcogenide switch device for stackable scalable 3D nanoscale memory. Nat Commun 4:2629. https://doi.org/10.1038/ncomms3629
10. Nandi SK, Liu X, Venkatachalam DK, Elliman RG (2015) Threshold current reduction for the metal–insulator transition in NbO2—x-selector devices: the effect of ReRAM integration. J Phys D. https://doi.org/10.1088/0022-3727/48/19/195105
11. Jo SH, Kumar T, Narayanan S, Lu WD, Nazarian H (2014) 3D-stackable crossbar resistive memory based on Field Assisted Superlinear Threshold (FAST) selector. In: 2014 IEEE international electron devices meeting. https://doi.org/10.1109/iedm.2014.7046999
12. Woo J, Lee D, Cha E, Lee S, Park S, Hwang H (2014) Control of Cu conductive filament in complementary atom switch for cross-point selector device application. IEEE Electron Device Lett 35(1):60–62. https://doi.org/10.1109/led.2013.2290120
13. Gopalakrishnan K, Shenoy RS, Rettner CT, Virwani K, Bethune DS, Shelby RM, Burr GW, Kellock A, King RS, Nguyen K, Bowers AN, Jurich M, Jackson B, Friz AM, Topuria T, Rice PM, Kurdi BN (2010) Highly-scalable novel access device based on Mixed Ionic Electronic conduction (MIEC) materials for high density phase change memory (PCM) arrays. In: Symposium on VLSI technology. https://doi.org/10.1109/VLSIT.2010.5556229.
14. Lin Q, Li Y, Xu M, Cheng Q, Qian H, Feng J et al (2018) Dual-layer selector with excellent performance for cross-point memory applications. IEEE Electron Device Lett 39(4):496–499. https://doi.org/10.1109/led.2018.2808465
15. Midya R, Wang Z, Zhang J, Savel'ev SE, Li C, Rao M et al (2017) Anatomy of Ag/hafnia-based selectors with 10(10)nonlinearity. Adv Mater. https://doi.org/10.1002/adma.201604457
16. Jeonghwan S, Jiyong W, Prakash A, Daeseok L, Hyunsang H (2015) Threshold selector with high selectivity and steep slope for cross-point memory array. IEEE Electron Device Lett 36(7):681–683. https://doi.org/10.1109/led.2015.2430332
17. Lee D, Kim T, Kim J, Sohn H (2020) Effect of Zr Addition on threshold switching characteristics of amorphous Ga_2Te_3 thin films. Phys Status Solidi. https://doi.org/10.1002/pssa.202000623
18. Ji X, Song L, He W, Huang K, Yan Z, Zhong S et al (2018) Super nonlinear electrodeposition-diffusion-controlled thin-film selector. ACS Appl Mater Interfaces 10(12):10165–10172. https://doi.org/10.1021/acsami.7b17235
19. He W, Yang H, Song L, Huang K, Zhao R (2017) A novel operation scheme enabling easy integration of selector and memory. IEEE Electron Device Lett 38(2):172–174. https://doi.org/10.1109/led.2016.2641018
20. Wang Z, Joshi S, Savelev SE, Jiang H, Midya R, Lin P et al (2017) Memristors with diffusive dynamics as synaptic emulators for neuromorphic computing. Nat Mater 16(1):101–108. https://doi.org/10.1038/nmat4756
21. Bricalli A, Ambrosi E, Laudato M, Maestro M, Rodriguez R, Ielmini D (2016) SiOx-based resistive switching memory (RRAM) for crossbar storage/select elements with high on/off ratio. In: IEEE international electron devices meeting (IEDM). https://doi.org/10.1109/IEDM.2016.7838344
22. Park JH, Kim D, Kang DY, Jeon DS, Kim TG (2019) Nanoscale 3D stackable Ag-doped HfOx-based selector devices fabricated through low-temperature hydrogen annealing. ACS Appl Mater Interfaces 11(32):29408–29415. https://doi.org/10.1021/acsami.9b08166
23. Yoo J, Kim SH, Chekol SA, Park J, Sung C, Song J et al (2019) 3D Stackable and scalable binary ovonic threshold switch devices with excellent thermal stability and low leakage current for high-density cross-point memory applications. Adv Electron Mater. https://doi.org/10.1002/aelm.201900196
24. Lee J, Kim J, Kim T, Sohn H (2021) Negative differential resistance characteristics in forming-free NbOx with crystalline NbO_2 phase. physica status solidi (RRL) – Rapid Res Lett 1:2. https://doi.org/10.1002/pssr.202000610
25. Song B, Xu H, Liu S, Liu H, Li Q (2018) Threshold Switching Behavior of Ag-SiTe-Based Selector Device and Annealing Effect on its Characteristics. IEEE J ELECTRON DEVI 6:674–679. https://doi.org/10.1109/jeds.2018.2836400
26. Tao Y, Li X, Xu H, Wang Z, Ding W, Liu W et al (2018) Improved uniformity and endurance through suppression of filament overgrowth in electrochemical metallization memory with AgInSbTe buffer layer. IEEE J Electron Device 6:714–720. https://doi.org/10.1109/jeds.2018.2843162
27. Abdul-Jabbar NM, Kalkan B, Huang GY, MacDowell AA, Gronsky R, Bourret-Courchesne ED et al (2014) The role of stoichiometric vacancy periodicity in pressure-induced amorphization of the Ga_2SeTe_2 semiconductor alloy. Appl Phys Lett. https://doi.org/10.1063/1.4892549
28. Kolobov AV, Fons P, Krbal M, Mitrofanov K, Tominaga J, Uruga T (2017) Local structure of the crystalline and amorphous states of Ga_2Te_3 phase-change alloy without resonant bonding: a combined x-ray absorption and ab initio study. Phys Rev B Condens Matter 95(5):054114. https://doi.org/10.1103/PhysRevB.95.054114

29. Dzhafarov TD, Khudyakov SV (1981) The influence of vacancies on silver diffusion in gallium phosphide. Phys Status Solidi 63(2):431–437. https://doi.org/10.1002/pssa.2210630208
30. Zhang S, Wu L, Song Z, Li T, Chen X, Yan S et al (2020) Breakthrough in high ON-state current based on Ag–GeTe8 selectors. J Mater Chem C 8(7):2517–2524. https://doi.org/10.1039/c9tc06673j
31. Imanishi Y, Kida S, Nakaoka T (2016) Direct observation of Ag filament growth and unconventional SET-RESET operation in GeTe amorphous films. AIP Adv 6(7):075003. https://doi.org/10.1063/1.4958633
32. Cho DY, Valov I, van den Hurk J, Tappertzhofen S, Waser R (2012) Direct observation of charge transfer in solid electrolyte for electrochemical metallization memory. Adv Mater 24(33):4552–4556. https://doi.org/10.1002/adma.201201499
33. Lim S, Woo J, Hwang H (2017) Communication—excellent threshold selector characteristics of Cu_2S-based atomic switch device. ECS J Solid State Sci Technol 6(9):P586–P588. https://doi.org/10.1149/2.0081709jss
34. Lee D, Kim T, Sohn H (2014) Highly reliable threshold switching behavior of amorphous Ga_2Te_3 films deposited by RF sputtering. Appl Phys Express. https://doi.org/10.7567/1882-0786/ab2cd9
35. Hermes C, Bruchhaus R, Waser R (2011) Forming-free TiO_2 -based resistive switching devices on CMOS-compatible W-plugs. IEEE Electron Device Lett 32(11):1588–1590. https://doi.org/10.1109/led.2011.2166371
36. Lv HB, Yin M, Zhou P, Tang TA, Chen BA, Lin YY, Bao A, Chi MH (2008) Improvement of endurance and switching stability of forming-free CuxO RRAM. In: Joint non-volatile semiconductor memory workshop and international conference on memory technology and design. https://doi.org/10.1109/NVSMW.2008.21
37. Song B, Cao R, Xu H, Liu S, Liu H, Li Q (2019) A HfO(2)/SiTe based dual-layer selector device with minor threshold voltage variation. Nanomaterials-Basel. https://doi.org/10.3390/nano9030408
38. Park JH, Kim SH, Kim SG, Heo K, Yu HY (2019) Nitrogen-induced filament confinement technique for a highly reliable hafnium-based electrochemical metallization threshold switch and its application to flexible logic circuits. ACS Appl Mater Interfaces 11(9):9182–9189. https://doi.org/10.1021/acsami.8b18970
39. Yoo J, Park J, Song J, Lim S, Hwang H (2017) Field-induced nucleation in threshold switching characteristics of electrochemical metallization devices. Appl Phys Lett 111(6):063109. https://doi.org/10.1063/1.4985165
40. Wang Z, Rao M, Midya R, Joshi S, Jiang H, Lin P et al (2018) Threshold switching of Ag or Cu in dielectrics: materials, mechanism, and applications. Adv Funct Mater 28(6):1704862. https://doi.org/10.1002/adfm.201704862
41. Wang W, Wang M, Ambrosi E, Bricalli A, Laudato M, Sun Z et al (2019) Surface diffusion-limited lifetime of silver and copper nanofilaments in resistive switching devices. Nat Commun 10(1):81. https://doi.org/10.1038/s41467-018-07979-0
42. Sun H, Liu Q, Li C, Long S, Lv H, Bi C et al (2014) Direct observation of conversion between threshold switching and memory switching induced by conductive filament morphology. Adv Funct Mater 24(36):5679–5686. https://doi.org/10.1002/adfm.201401304
43. Chae BG, Seol JB, Song JH, Baek K, Oh SH, Hwang H et al (2017) Nanometer-scale phase transformation determines threshold and memory switching mechanism. Adv Mater. https://doi.org/10.1002/adma.201701752

Publisher's Note